



INSTITUT DE FRANCE  
Académie des sciences

# Comptes Rendus

---

## Géoscience

*Sciences de la Planète*

Qing Shi and Nianqiao Fang


**Petrogenesis and tectonic significance of mafic–ultramafic rocks from Southwest Yunnan, China**

Volume 352, issue 8 (2020), p. 589-599

Published online: 4 November 2020

Issue date: 27 January 2021

<https://doi.org/10.5802/crgeos.15>

 This article is licensed under the  
CREATIVE COMMONS ATTRIBUTION 4.0 INTERNATIONAL LICENSE.  
<http://creativecommons.org/licenses/by/4.0/>



*Les Comptes Rendus. Géoscience — Sciences de la Planète sont membres du  
Centre Mersenne pour l'édition scientifique ouverte*

[www.centre-mersenne.org](http://www.centre-mersenne.org)

e-ISSN : 1778-7025



Original Article — Tectonics, Tectonophysics

# Petrogenesis and tectonic significance of mafic–ultramafic rocks from Southwest Yunnan, China

Qing Shi<sup>a</sup> and Nianqiao Fang<sup>\*, a</sup>

<sup>a</sup> China University of Geosciences (Beijing), No.29 Xueyuan Road, 100083, Beijing, P.R. China

E-mails: sq910924@sina.com (Q. Shi), fangnq@foxmail.com, fangnq@yeah.net (N. Fang)

**Abstract.** This study focuses on the mafic–ultramafic lavas of the Early Carboniferous outcrop in Mangxin, southwestern Yunnan, China. Picrites with 26–32 wt% MgO and a quenched texture are the most significant components of this rock association. This article divides the Mangxin picrites into two types. The mantle potential temperature ( $T_p$ ) of these picrites is higher than the  $T_p$  range of mid-ocean ridges and reaches that of mantle plumes. According to the geochemical characteristics, the Type-1 picrites probably formed from the melting of the mantle plume head and were contaminated by ambient depleted mantle, whereas the Type-2 picrites formed from the melting of mantle plume tails. These plume-related mafic–ultramafic rocks in Mangxin and the ocean island basalt (OIB)-carbonate rock associations in many areas of the Changning–Menglian belt provide significant evidence for the improvement of previous models of the Palaeotethyan oceanic plateau.

**Keywords.** Picrite, Mantle plume, Mantle potential temperature, Oceanic plateau, Palaeotethys.

*Manuscript received 15th August 2018, revised 12th November 2018 and 19th April 2019, accepted 21st July 2020.*

## 1. Introduction

Ultramafic lavas are generated by high degrees of partial melting (>10–15%) in the mantle [Herzberg and O'Hara, 2002]. These lavas are an unusual type of Phanerozoic volcanics and have drawn the attention of many researchers [Arndt and Nisbet, 1982, Arndt et al., 2008, Herzberg and O'Hara, 2002]. Several classic studies have revealed that ultramafic

lavas such as picrites and komatiites may be produced by the fractional melting of a mantle plume [Arndt and Weis, 2002, Arndt et al., 1997]. Hawaii is the most typical example of such a system: its intraplate ocean island rock association of picrites, alkali and tholeiitic basalts with high mantle potential temperatures indicate a plume origin [Herzberg and Asimow, 2015, Putirka et al., 2011]. The Cretaceous komatiites of Gorgona Island were explained as products of the head of a mantle plume by Arndt et al. [1997] and Kerr et al. [1997]. The picrites of Baffin Island and West Greenland were interpreted to be associated with the Tertiary Icelandic plume

\* Corresponding author.

[Herzberg and O'Hara, 2002, Larsen and Pedersen, 2000]. Although we cannot ignore picritic magmas that were produced by island-arc regimes, such as the Aleutians, Kamchatka, Solomon Islands and Canada [Cameron and Nisbet, 1982, Kamenetsky et al., 1995, Milidragovic et al., 2016, Schuth et al., 2004], the preferred tectonic environment of ultramafic lavas is still related to mantle plumes based on the abnormal thermal conditions that are required by their high-Mg characteristics [Herzberg and O'Hara, 1998, Thompson et al., 2001].

Western Yunnan, China, is a region that has not attracted much research attention. Mafic and ultramafic lavas widely outcrop in this region, and the MgO contents of alkali basalts consistently reach 8–14% while picrite pillows that outcrop at Xiaohaijiang have MgO contents of 35–40%. The picritic rock association that outcrops at Mangxin discussed in this article belong to the Devonian to Triassic Palaeotethys orogenic belt, which is a different tectonic region from the Emeishan large igneous province (LIP). The picrites in Mangxin usually have an MgO content of 26–32% (loss on ignition (LOI)-free), and together with the local high-Mg accumulative peridotites and basalts, these rocks represent the largest and most diverse volcanic eruption on record in West Yunnan. Fang and Feng [1996] reported that these rocks represented the products of an ancient LIP in the Palaeotethys. Zhang and Zhu [1995] considered the Mangxin picrites to represent the failed accumulative rock that erupted in a mid-ocean ridge (MOR) environment. Zhong [1998] argued that these rocks were similar to Hawaiian picrites and were related to an oceanic island environment. Fang and Niu [2003] considered Mangxin picrites to have formed under high-temperature melting conditions. The purpose of this article is to utilize this rare geological record of Mangxin picrites, further analyse their characteristics, and discuss their petrogenesis and tectonic significance.

## 2. Geological background

Many previous studies have shown that the Changning–Menglian belt in western Yunnan, China, was the main basin of the Palaeotethyan archipelagic ocean [Fang et al., 1994, Liu et al., 1993, Zhong, 1998]. Mangxin, the study area, is located at the southern end of the Changning–Menglian belt in

China. This area contains abundant outcrops of Late Palaeozoic mafic–ultramafic pillow lavas, radiolarian chert, manganese rocks and dolomitic pure carbonate rocks, thus providing an important window for understanding the evolution of the Palaeotethys. The samples were collected from the region to the south of Mangxin and included picrites, accumulative peridotites and basalts. Detailed information about the geological background, sampling sites, analytical methods and data can be found in the Supplementary materials.

## 3. Petrological and geochemical characteristics of the samples

The picrites in Mangxin generally exhibit quenched textures in their matrices. These rocks can be divided into two different types based on their structures and compositions. The Type-1 samples (MX01, MX02, MX03, and MX04) are pillowed picrites with obvious porphyritic textures. Euhedral to subhedral olivine phenocrysts (0.1–3 mm) and few Cr-spinels are observed. The matrix mainly consists of skeletal-acicular clinopyroxenes and plagioclases as well as aphanitic alteration products. The average matrix compositions (LOI-free) of SiO<sub>2</sub> (47–48 wt%) and MgO (8–11 wt%) are similar to those of basaltic magma. Vesicles are visible (Figure 1a). The Type-2 samples (MX05 and MX06) are pillowed picrites with obvious porphyritic textures. Many euhedral olivines (0.1–2 mm) with clear edges and few Cr-spinels are observed. The matrix mainly consists of tiny feather-shaped pyroxenes and some aphanitic materials. No plagioclase is observed. The average matrix composition (LOI-free) of SiO<sub>2</sub> (41–43 wt%) and MgO (21–23 wt%) is similar to that of picritic magma. Fewer vesicles are visible (Figure 1b). Although the classification of these two picrite types is similar to that reported by Fang and Niu [2003], the samples presented here were newly collected in 2013–2015 from different outcrops than those sampled by Fang and Niu [2003]. The accumulative peridotites in this area (AP01, AP02) have been significantly altered. The olivines and clinopyroxenes form a cumulate texture. Most of the olivines are subhedral and have abundant fractures that are filled with serpentinite and chlorite. The clinopyroxenes occur as anhedral grains in the gaps between olivines. Some Cr-spinels are visible.

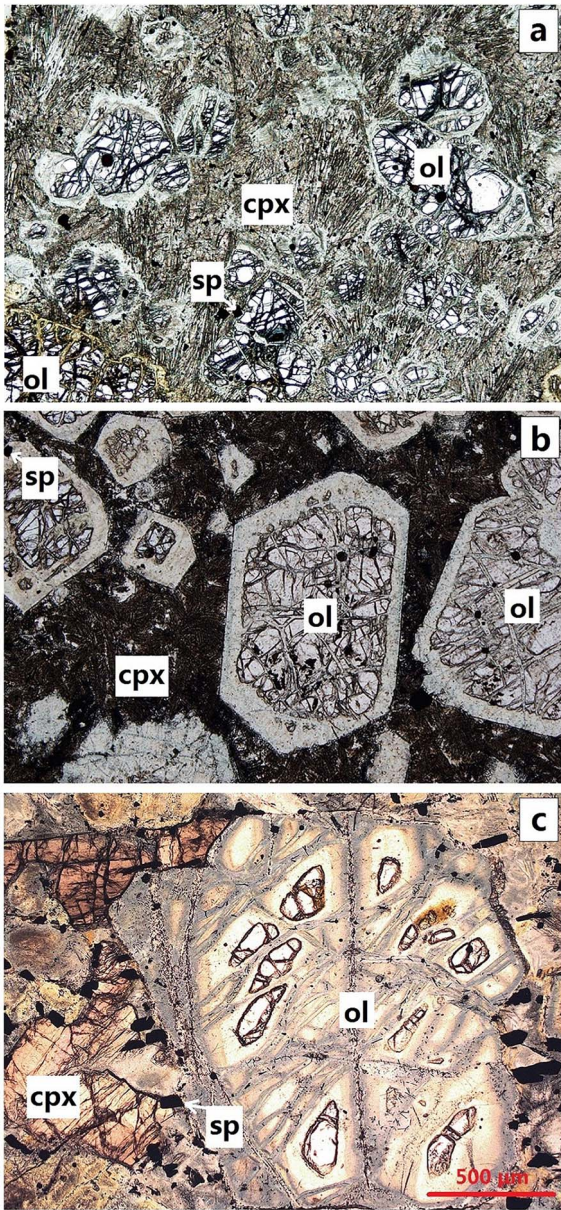


**Figure 1.** Photomicrographs of picrite and accumulative peridotite samples from Mangxin under single-polarized light: (a), Type-1 picrite; (b), Type-2 picrite; (c), accumulative peridotite; ol, olivine; cpx, clinopyroxene; and sp, Cr-spinel.

No quenched matrixes or vesicles are observed (Figure 1c). The whole-rock compositions of the picrites and the accumulative peridotites are similar. The  $\text{SiO}_2$  contents of these ultramafic rocks are 43.56–

47.50% (wt%) (LOI free), and the MgO contents reach 26.35–32.31% (wt%). This high-Mg characteristic is similar to that of komatiites (MgO > 18%), but these samples did not contain “spinfex olivine” [Arndt and Nisbet, 1982]. Therefore, we refer to them as “high-magnesium picrites” in the following discussion. This high-Mg characteristic indicates an accumulation of olivine.

The basalts in this area can also be divided into two types based on their chemical compositions. The high-Ti basalts have higher  $\text{TiO}_2$  contents (3.17–3.87 wt%) but lower  $\text{Al}_2\text{O}_3$  (12.93–14.94 wt%) and CaO (5.73–9.10 wt%) contents (LOI free). Their matrices consist of acicular plagioclases and granular clinopyroxenes, and the former are more prevalent than the latter. The acicular plagioclases are directionally arranged in some samples, indicating the flow of magma. Both plagioclase and clinopyroxene phenocrysts (0.5–1 mm) are observed. The low-Ti basalts have lower  $\text{TiO}_2$  (1.07–1.82 wt%) contents but higher  $\text{Al}_2\text{O}_3$  (9.84–19.81 wt%) and CaO (8.22–14.73 wt%) contents (LOI free). Their matrices consist of tiny plagioclases and clinopyroxenes, and the latter are more prevalent than the former. Many clinopyroxene phenocrysts (0.5–2 mm) and vesicles are observed. A pillow structure is found in both types, confirming that they erupted in the same deep-sea environment as the picrites.

The  $\text{SiO}_2$  content of the Mangxin basalts is positively correlated with MgO (Figure 2a), whereas the  $\text{SiO}_2$  and FeO contents in the Mangxin ultramafic rocks and the  $\text{Al}_2\text{O}_3$  and  $\text{TiO}_2$  contents in all of the samples are negatively correlated with the MgO content (Figures 2a–d). There is no obvious correlation between FeO and MgO in the Mangxin basalts (Figure 2b). The ultramafic rocks can also be divided into two categories as basalts according to the  $\text{TiO}_2$  contents: the Type-1 picrites have lower  $\text{TiO}_2$  contents (0.51–0.56 wt%), whereas the Type-2 picrites and accumulative peridotites have higher  $\text{TiO}_2$  contents (0.97–1.19 wt%) (Figure 2d). The Mangxin samples have experienced some alteration, and the values of the loss on ignition (LOI) vary between 2.49 and 10.09 wt%. There is a negative correlation between LOI and Mg# in both the picrites and basalts, indicating that the alteration leads to a small decrease in Mg#.

The Type-1 picrites are depleted in light rare earth elements (REEs) and exhibit similar patterns to those

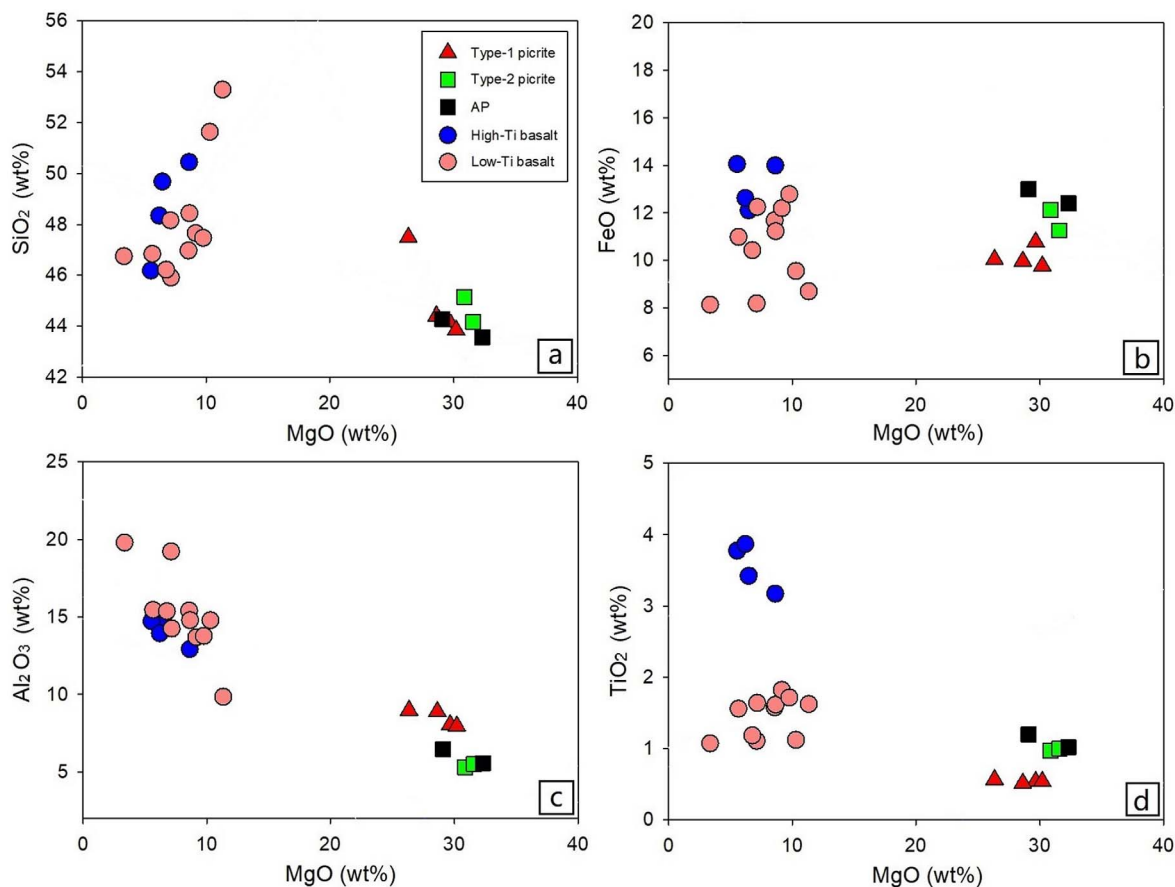


**Figure 2.** Plots of certain major elements versus MgO for the Mangxin picrites, accumulative peridotites and basalts: (a), SiO<sub>2</sub> (wt%); (b), FeO<sup>T</sup> (wt%); (c), Al<sub>2</sub>O<sub>3</sub> (wt%); (d), TiO<sub>2</sub> (wt%) vs MgO (wt%). The total iron is expressed as FeO; AP, accumulative peridotites.

of N-MORB; in particular, the curve of sample MX01 perfectly matches the curve of N-MORB except for the negative Ce anomaly, which could be related to the alteration of olivine [Frisby et al., 2016, Niu, 2004]. The Type-2 picrites and accumulative peridotites are enriched in light REEs and exhibit similar patterns to those of OIB, although their values are lower (Figure 3a). The trace element spider diagrams also show that the patterns of the Type-1 picrites are similar to those of N-MORB but with more negative anomalies of Ta, Ti, Zr and Hf and positive anomalies of Pb. The curves of the Type-2 picrites and accumulative peridotites are similar to those of OIB except for the obvious negative anomalies of Ba, K and Sr. These anomalies reflect the alteration of the samples (Figure 3b). The two types of basalt in the Mangxin

area have similar REE patterns to those of ultramafic rocks (Figure 3c): the high-Ti basalts are enriched in light REEs and exhibit similar patterns to those of OIBs, whereas the low-Ti basalts have flat curves and exhibit similar patterns to those of E-MORB (more enriched in light REEs than N-MORB). The negative anomalies of Rb, K and Sr in the high-Ti basalts also indicate alteration (Figure 3d).

## 4. Discussion

### 4.1. Calculation of mantle potential temperature

In recent years, the topic of mantle plumes has attracted considerable attention. The concept of mantle potential temperature ( $T_p$ ) was proposed to



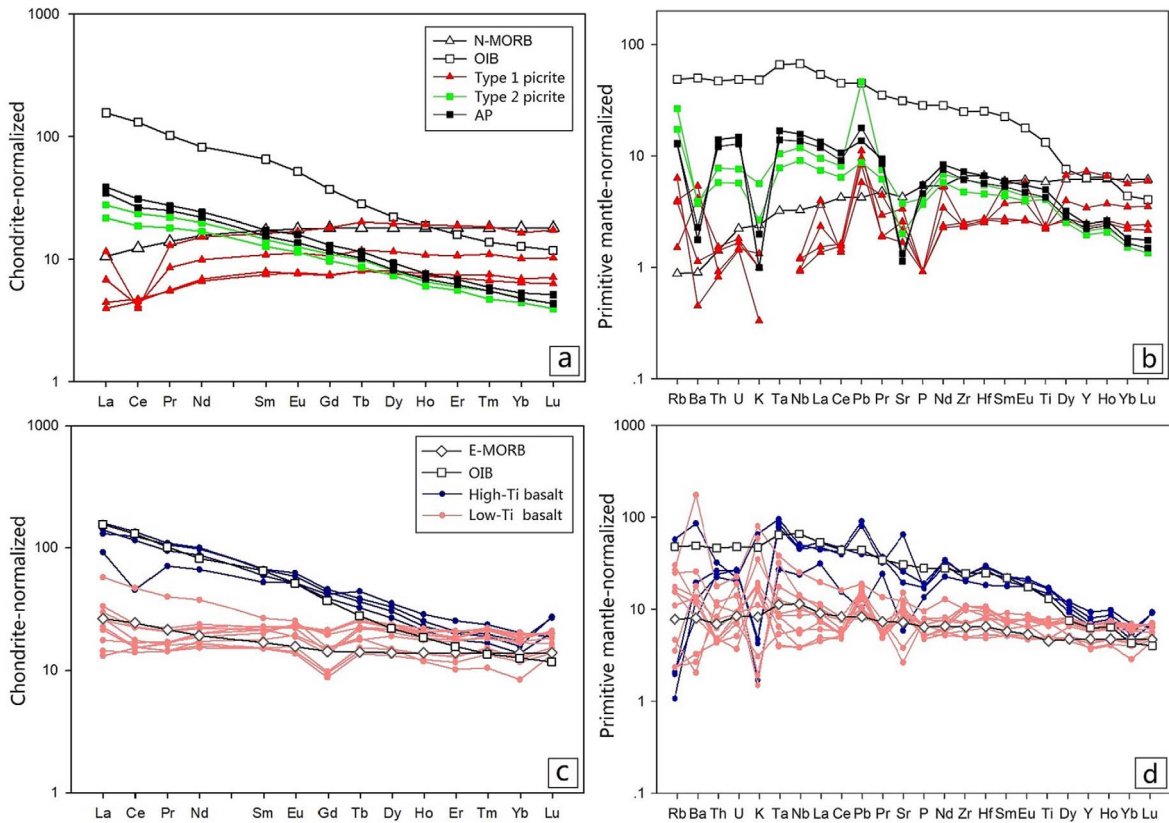


**Figure 3.** Chondrite-normalized REE patterns and primitive mantle-normalized trace element diagrams of the Mangxin samples: (a) and (b), ultramafic rocks; and (c) and (d), basalts. The normalization values, average OIB, N-MORB and E-MORB compositions are from Sun and McDonough [1989].

discuss the thermal anomalies in different regions of the mantle. According to different researchers, a clear distinction in  $T_p$  exists between MORs and hot spots affected by mantle plumes. The  $T_p$  values of MORs are 1280–1450 °C [Asimow et al., 2001, Herzberg and O’Hara, 2002, McKenzie and Bickle, 1988, McKenzie et al., 2005, Putirka, 2008]. The  $T_p$  of Iceland is higher, at approximately 1480–1553 °C. The  $T_p$  of Ontong Java Plateau is 1482–1534 °C. The  $T_p$  of Hawaii (Mauna Kea), which is widely regarded as a plume-affected oceanic island, reaches 1526–1549 °C. The  $T_p$  of Gorgona Island in the Caribbean LIP is 1539–1596 °C [Herzberg and Asimow, 2015, MacLennan et al., 2001]. Thus, plume-associated regions generally have higher  $T_p$  values, we therefore hope to predict the probable plume influence by calculating the  $T_p$  of the Mangxin area.

To calculate the  $T_p$ , we must determine if the

olivines represent mantle xenocrysts or are of magmatic origin. Only the latter can be used for the calculation. Most of the olivines in the Mangxin picrites are euhedral with clear edges and no zonal textures. According to Thompson and Gibson [2000], mantle olivines always have CaO contents below 0.1% (wt%), whereas magmatic olivines have CaO contents above 0.1% (wt%). Gavrilenko et al. [2016] showed that olivines that crystallized from a parental magma with high H<sub>2</sub>O content (i.e., arc systems) always have low Ca contents (approximately 1000 ppm). The olivines in the Mangxin picrites generally have CaO contents of 0.2–0.3% (wt%), indicating an anhydrous magmatic origin. In addition, xenocrysts from the mantle always have kink bands because of the high pressure [Thompson and Gibson, 2000]. No kink bands were observed in the Mangxin picrites, which also eliminates the possibility that these olivines are man-

tle xenocrysts.

Wan et al. [2008] provided a new Al-in-olivine thermometer to determine the minimum crystallization temperature ( $T_c$ ). This thermometer is more reliable because it is largely independent of the melt composition, H<sub>2</sub>O content and influences from olivine crystallization or accumulation. Coogan et al. [2014] improved this thermometer to expand its calibration range. The olivines in the Mangxin Type-1 picrites generally have higher Al<sub>2</sub>O<sub>3</sub> and Fo values than the Type-2 samples. Compared with those in other regions, the olivines in the Type-1 picrites plot in a similar area as the olivines from the Siqueiros MORB and Gorgona komatiite in the Al<sub>2</sub>O<sub>3</sub>–Fo diagram, whereas the olivines in the Type-2 picrites plot in a similar area as the olivines from Hawaii basalt (Figure 4a).

We used the improved Al-in-olivine thermometer from Coogan et al. [2014] to calculate the average  $T_c$  of the Type-1 (1363 °C for MX01, 1417 °C for MX02 and 1332 °C for MX03) and Type-2 picrites (1404 °C for MX05 and 1399 °C for MX06). The Fo–T diagram (Figure 4b) of the olivines also shows the differences between the two types of Mangxin picrites. Coogan et al. [2014] contrasted the results of Al-in-olivine thermometry to those of other thermometers to assess the calculations' accuracy. Their results were consistent with the olivine crystallization temperatures calculated by Herzberg and O'Hara [2002]. For example, the  $T_c$  of the Siqueiros MORB from Herzberg and O'Hara [2002] was 1277–1301 °C, which was only slightly higher than that from Al-in-olivine thermometry (1270 °C). Similar results were obtained for the Baffin Island basalts (1337–1445 °C vs 1408 °C) and Gorgona komatiites (1371–1457 °C vs 1435 °C). Thus, the results of Al-in-olivine thermometry are reliable. The calculated  $T_c$  values of the Mangxin picrites are higher than those of the Siqueiros MORB and similar to those of the Baffin Island basalts and Gorgona komatiites (Figure 4b). Notably, the  $T_c$  from this approach is unlikely to exactly match the liquidus temperature, but the results should be very close to the liquidus temperature, and the difference may be within a few tens of degrees [Coogan et al., 2014].

For comparison, it is desirable to estimate the liquidus temperature from the MgO content of the liquid. The olivine-liquid Mg–Fe distribution coefficient ( $K_D$ ) is relatively constant between 0.3 and 0.34 and

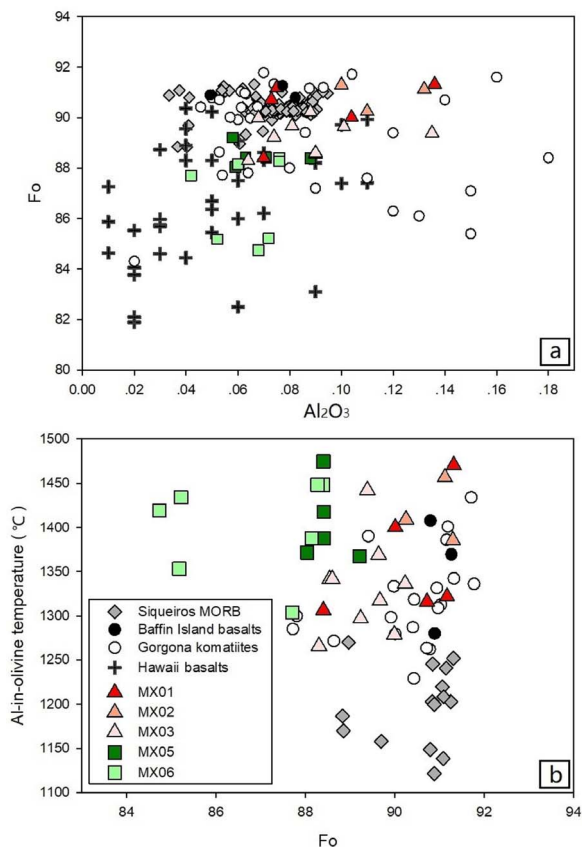


**Figure 4.** Diagrams of Al-in-olivine temperature: (a), olivine Al<sub>2</sub>O<sub>3</sub> content versus olivine Fo; (b), olivine Fo versus Al-in-olivine temperature. The Siqueiros data are from Putirka et al. [2011] and Coogan et al. [2014]; the Baffin Island data are from Coogan et al. [2014]; the Gorgona data are from Echeverría [1980] and Coogan et al. [2014]; and the Hawaii data are from Sobolev and Nikogosyan [1994], Rhodes [1995] and Baker et al. [1996].

increases with pressure [Putirka, 2005, Roeder and Emslie, 1970]; therefore, we can estimate the MgO content of the liquid based on the composition of the olivine. For the Mangxin picrites, we used a  $K_D$  of 0.33 [Arndt and Nisbet, 1982] and the highest forsterite contents that were measured in olivines from each sample. The calculation was performed on the anhydrous whole-rock composition assuming that the FeO content was constant during crystallization. Our calculation suggests that the parental magma

**Table 1.** Minimum crystallization temperatures and mantle potential temperatures of MORB, LIP and the Mangxin picrites

	Mangxin Type-1 picrite			Mangxin Type-2 picrite		MORB	LIP
	MX01	MX02	MX03	MX05	MX06		
$T_c$ (°C)	1363	1417	1332	1404	1399	1270–1301	1337–1457
$T_p$ (°C)	1465	1513	1437	1502	1497	1280–1450	1450–1600

The  $T_c$  and  $T_p$  values of MORB and LIP are summarized from Asimow et al. [2001], Coogan et al. [2014], Herzberg and O'Hara [2002], Herzberg et al. [2010], McKenzie and Bickle [1988], McKenzie et al. [2005], Milidragovic et al. [2016], Putirka [2008].

of the Mangxin picrites had a MgO content of 20.72 wt% (MX01), 18.79 wt% (MX02), 16.82 wt% (MX03), 18.34 wt% (MX05) and 15.73 wt% (MX06). The amount of cumulus olivine in the Mangxin picrites varies from 30% to 50% according to a comparison with the whole-rock MgO composition. Then, the liquidus temperature, which is constrained by the relationship  $T$  (°C) = 20 \* MgO + 1000 [Arndt and Nisbet, 1982], varies from 1314 °C to 1414 °C, which is consistent with the value from the Al-in-olivine thermometer.

The  $T_p$  of the Mangxin picrites can be estimated by the approach of Putirka [2005] and the formula for the solidus of McKenzie and Bickle [1988]. The  $T_p$  values for the Type-1 (1465 °C for MX01, 1513 °C for MX02 and 1437 °C for MX03) and Type-2 picrites (1502 °C for MX05 and 1497 °C for MX06) are calculated with a melt fraction in oceanic islands of 0.2 [Walter, 1998]. The  $T_p$  of the ambient mantle, which feeds MOR basalt volcanism, is 1280–1450 °C, and the  $T_p$  of Phanerozoic intraplate basalts is 1450–1600 °C; these differences are attributed to anomalous thermal plumes (Asimow et al., 2001, Herzberg and O'Hara, 2002, Herzberg et al., 2010, McKenzie et al., 2005, Milidragovic et al., 2016, Putirka, 2008). The  $T_p$  of the Mangxin picrites is generally within the  $T_p$  range of mantle plumes (Table 1).

#### 4.2. Information from high field-strength elements

The contents and ratios of certain immobile high field-strength elements (e.g., Th, Nb, Zr, Yb, Y, Hf, Ta and Ti) are suitable for tracking the origin of old basalt samples because these elements are not affected by secondary alteration and do not change over time, unlike isotope ratios [Condie, 2005]. The

mantle is inhomogeneous, and several end-members have been divided based on their different isotope and trace element compositions. All types of mantle-derived magma can be explained by the mixing of these end-members. With the exception of PM (primitive mantle), Condie [2005] divided 4 different end-members of oceanic mantle: DEP (deep plume component), EN (enriched component), REC (recycled component) and DM (shallow depleted mantle component). He compared samples from several plume-affected areas, such as the Caribbean Plateau, Kerguelen Plateau and Hawaii, and found that the basalts derived from plume heads had a mixed source of EN and DEP (plot between EN and DEP), whereas the basalts derived from plume tails were related to REC (plot near REC). However, one exception was observed: the picrites and komatiites that erupted on Gorgona Island were produced by a high degree of melting of the plume head [Révillon et al., 2000], although most of them plotted in the N-MORB area (near DM) in the Zr/Y–Nb/Y diagram. These rocks originated from an extremely depleted source that was unclear but similar to DM [Condie, 2005].

In the Zr/Y–Nb/Y diagram (Figure 5a), most of the Mangxin basalts plot in the areas of OIBs and oceanic plateau basalts. Most of the high-Ti basalts plot near REC (related to plume tails), and the low-Ti basalts plot between EN and DEP (related to plume heads). Furthermore, the high-Ti basalts have higher TiO<sub>2</sub> contents and higher Ti/Y ratios (>500) than the low-Ti basalts, which is consistent with the high-Ti basalts being from a plume tail and the low-Ti basalts being from a plume head within the Emeishan LIP [Xu et al., 2004]. The Type-2 picrites and accumulative peridotites plot near high-Ti basalts and thus near REC, whereas most of the Type-1 picrites plot near



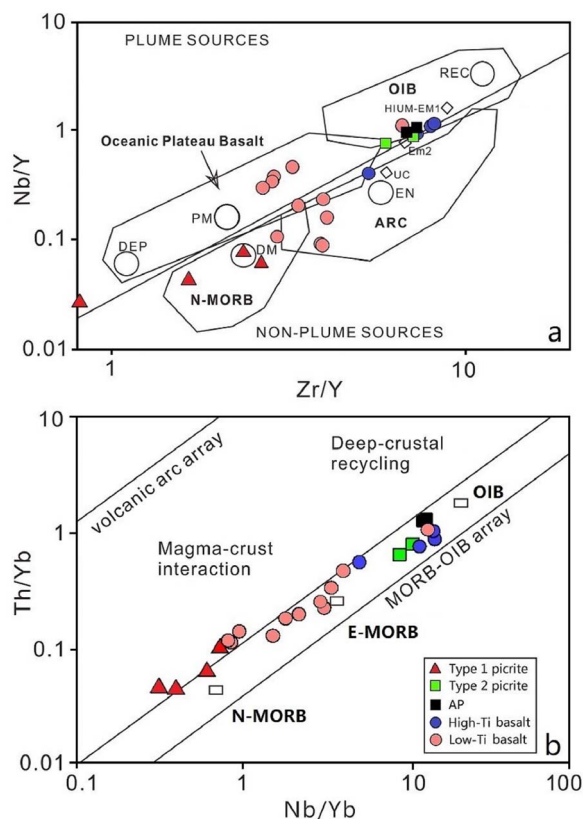


**Figure 5.** High field-strength element diagrams of Mangxin samples: a, Zr/Y–Nb/Y diagram; b, Nb/Yb–Th/Yb diagram: UC, upper continental crust; EM1 and EM2, enriched mantle sources; HIMU, high U/Pb source; PM, primitive mantle; DM, shallow depleted mantle; DEP, deep plume component; EN, enriched component; REC, recycled component; ARC, arc-related basalts; N-MORB, normal ocean ridge basalts; E-MORB, enriched ocean ridge basalts; OIB, oceanic island basalts [Condie, 2005, Pearce, 2008].

DM, which is similar to the characteristics of the picrites and komatiites from Gorgona.

In addition, the Nb/Yb–Th/Yb diagram (Figure 5b) from Pearce [2008] shows similar results. Oceanic basalts, including OIB, E-MORB and N-MORB, are expected to plot within the MORB-OIB array in the Nb/Yb–Th/Yb diagram, whereas the lavas, with continental crust or subduction components, are expected to plot above the array. As shown in Fig-

ure 5b, most of the Mangxin samples plot within the MORB-OIB array, suggesting that they are not arc-related. Most of the high-Ti basalts, Type-2 picrites and accumulative peridotites plot near OIB, whereas most of the low-Ti basalts plot near E-MORB, and the Type-1 picrites plot near N-MORB; these plot locations are consistent with the characteristics of the REE patterns.

#### 4.3. Speculation about the petrogenesis of the mafic–ultramafic rocks in Mangxin

According to the previous analysis, the  $T_p$  of the Type-1 picrites calculated by the Al-in-olivine thermometer matched the  $T_p$  range of mantle plumes. These rocks had the same low-TiO<sub>2</sub> characteristic as the Mangxin low-Ti basalts, which may reflect a plume head origin. The characteristics apparent in the Zr/Y–Nb/Y diagram (near DM) and the Nb/Yb–Th/Yb diagram (near N-MORB) suggest that the Type-1 picrites were contaminated by magma from a depleted source (i.e., ambient depleted mantle) during their eruption, which is also reflected in their depleted REE patterns. It is also possible that a depleted part of the plume head source existed; however, further studies are needed to discuss this possibility in detail. The  $T_p$  of the Type-2 picrites was also within the  $T_p$  range of mantle plumes. The OIB-type REE and trace element patterns of accumulative peridotite were similar to those of the Type-2 picrites, indicating that they had a similar magma source. The identical characteristics of the Mangxin Type-2 picrites, accumulative peridotites and high-Ti basalts in the Zr/Y–Nb/Y and Nb/Yb–Th/Yb diagrams reflect their deep plume tail origin. It is also worth mentioning that high-Ti and low-Ti suites are typical classifications of continental flood-basalts (CFBs); therefore, based on the archipelago setting, the possibility of continental crust contamination of Mangxin basalts may also exist.

#### 4.4. Speculation about a possible oceanic plateau in Palaeotethys

To summarize, in the Mangxin area, (1) the formation of Type-1 picrites and low-Ti basalts might have been related to the melting of the mantle plume head; (2) the formation of Type-2 picrites and high-Ti

basalts might have been related to the mantle plume tail (or core); and (3) the accumulative peridotites formed from a similar magma as the Type-2 picrites in the magma chambers. Thus, we speculate that an oceanic plateau caused by a mantle plume might have been present in the basin of Palaeotethys. This hypothesis is based on the geological background of the study area. The wide distribution of OIB-pure carbonate associations in the study area is notable. This kind of rock association outcrops in Yongde, Zhenkang, Gengma, Shuangjiang, Cangyuan, Lancang and Menglian in western Yunnan, covers more than 40% of the Changning–Menglian belt and is often accompanied by radiolarian siliceous rocks, manganese rocks and phosphate rocks. There have been numerous disputes about the tectonic environment represented by this rock association, such as rift, seamounts, island chain, arc or oceanic plateau. Based on the following facts: (1) Most of the basalts are OIBs. The purity of the early Carboniferous-early Permian limestone overlying the basalts is very high (wt% > 96% CaCO<sub>3</sub>). Their coexistence precludes a continental background, such as rift or arc [Liu et al., 1993]. (2) The age of the sedimentary interlayers in the volcanic rocks is early Carboniferous (Tournaisian) [Feng et al., 1997, Zhang and Feng, 2002]. Large-scale magmatic activity occurred during the same period, which precludes isolated seamounts and the possibility of forming seamount chains with plate drift. Fang et al. [1998] speculated that there should be a large area of oceanic plateau in the main basin of Palaeotethys, and the formation mechanism may be the role of large igneous province. This may currently be the most reasonable interpretation of the origin of the OIB-limestone association; it has gained the recognition of many researchers, but it also requires additional evidence. In particular, in the LIP system inferred by Fang, the ultramafic rocks are not clearly positioned. The monographic study of the Mangxin picrites, accumulative peridotites and two types of basalts undoubtedly provide significant evidence for the improvement of the previous model for the Palaeotethyan oceanic plateau.

## 5. Conclusions

(1) The mantle potential temperature ( $T_p$ ) of Type-1 and Type-2 picrites in Mangxin as calculated by Al-in-olivine thermometry is 1437–1513 °C and 1497–

1502 °C, respectively, which is within the  $T_p$  range of mantle plumes. The Type-1 picrites formed from the melting of the mantle plume head. The Type-2 picrites and accumulative peridotites formed from picritic magma that was produced by the mantle plume tail (or core), with the former erupting underwater, and the latter accumulating in magma chambers.

(2) The Type-1 picrites had the REE, trace element and high field-strength element characteristics of N-MORB, indicating possible contamination of the ambient depleted mantle and/or a relatively high melt fraction of the plume head. The Type-2 picrites and accumulative peridotites exhibited the REE, trace element and high field-strength element characteristics of OIB.

(3) The basalts in the Mangxin area could be divided into two types based on the chemical compositions and the characteristics of their REE patterns and high field-strength elements. The high-Ti basalts were similar to OIB and formed from the melting of the plume tail (or core), whereas the low-Ti basalts were similar to E-MORB and formed from the melting of the plume head.

(4) The existence of plume-related mafic-ultramafic rocks in Mangxin and the OIB-carbonate associations in many areas of the Changning–Menglian belt provide significant evidence for the improvement of the previous model for the Palaeotethyan oceanic plateau.

## Acknowledgements

We are grateful to Dejan Milidragovic and Nicholas Arndt for performing a critical review of the manuscript. This work was supported by the National Natural Science Foundation of China (No. 41276047; No. 40876029).

## Supplementary data

Supporting information for this article is available on the journal's website under <https://doi.org/10.5802/crgeos.15> or from the author.

## References

- Arndt, N. T., Kerr, A. C., and Tarney, J. (1997). Dynamic melting in plume heads: the formation of Gorgona komatiites and basalts. *Earth Planet. Sci. Lett.*, 146(1):289–301.

- Arndt, N. T., Leshner, C. M., and Barnes, S. J. (2008). *Komatiites*. Cambridge University Press, Cambridge.
- Arndt, N. T. and Nisbet, E. G. (1982). *Komatiites*. George Allen and Unwin, London.
- Arndt, N. T. and Weis, D. (2002). Oceanic plateaus as windows to the Earth's interior: An ODP success story. *Joedes J.*, 28(1):79–84.
- Asimow, P. D., Hirschmann, M. M., and Stolper, E. M. (2001). Calculation of peridotite partial melting from thermodynamic models of minerals and melts, IV. Adiabatic decompression and the composition and mean properties of mid-ocean ridge basalts. *J. Petrol.*, 42:963–998.
- Baker, M. B., Sophie, A., and Stolper, E. M. (1996). Petrography and petrology of the Hawaii Scientific Drilling Project lavas: Inferences from olivine phenocryst abundances and compositions. *J. Geophys. Res. Solid Earth*, 101(B5):11715–11727.
- Cameron, W. E. and Nisbet, E. G. (1982). Phanerozoic analogues of komatiitic basalts. In Arndt, N. T. and Nisbet, E. G., editors, *Komatiites*, pages 29–50. George Allen and Unwin, London.
- Condie, K. C. (2005). High field strength element ratios in Archean basalts: a window to evolving sources of mantle plumes? *Lithos*, 79:491–504.
- Coogan, L. A., Saunders, A. D., and Wilson, R. N. (2014). Aluminum-in-olivine thermometry of primitive basalts: Evidence of an anomalously hot mantle source for large igneous provinces. *Chem. Geol.*, 368:1–10.
- Echeverría, L. M. (1980). Tertiary or Mesozoic komatiites from Gorgona Island, Colombia: Field relations and geochemistry. *Contribut. Mineral. Petrol.*, 73(3):253–266.
- Fang, N. Q. and Feng, Q. L. (1996). *Devonian to Triassic Tethys in western Yunnan, China*. China University of Geosciences Press, Wuhan.
- Fang, N. Q., Feng, Q. L., Zhang, S. H., and Wang, X. L. (1998). Paleo-Tythes evolution recorded in Changning–Menglian Belt, Western Yunnan, China. *C. R. Acad. Sci. Paris*, 326(Ser. IIa):275–282.
- Fang, N. Q., Liu, B. P., and Feng, Q. L. (1994). Late Paleozoic and Triassic deep-water deposits and tectonic evolution of the Paleo-Tethys in the Changning–Menglian and Lancangjiang belts, southwestern Yunnan. *J. Southeast Asian Earth Sci.*, 9:374–463.
- Fang, N. Q. and Niu, Y. L. (2003). Late palaeozoic ultramafic lavas in Yunnan, SW China, and their geodynamic significance. *J. Petrol.*, 44(1):141–157.
- Feng, Q. L., Ye, M., and Zhang, Z. J. (1997). Early Carboniferous Radiolarians from western Yunnan. *Acta Micropalaeontol. Sin.*, 14(1):79–92.
- Frisby, C., Bizimis, M., and Mallick, S. (2016). Seawater-derived rare earth element addition to abyssal peridotites during serpentinization. *Lithos*, 248:432–454.
- Gavrilenko, M., Herzberg, C., Vidito, C., Carr, M. J., Tenner, T., and Ozerov, A. (2016). A calcium-in-olivine geohygrometer and its application to subduction zone magmatism. *J. Petrol.*, 57(9):1811–1832.
- Herzberg, C. and Asimow, P. D. (2015). PRIMELT3 MEGA.XLSM software for primary magma calculation: Peridotite primary magma MgO contents from the liquidus to the solidus. *Geochem. Geophys. Geosyst.*, 16(2):563–578.
- Herzberg, C., Condie, K., and Korenaga, J. (2010). Thermal history of the Earth and its petrological expression. *Earth Planet. Sci. Lett.*, 292:79–88.
- Herzberg, C. and O'Hara, M. J. (1998). Phase equilibrium constraints on the origin of basalts, picrites, and komatiites. *Earth Sci. Rev.*, 44:39–79.
- Herzberg, C. and O'Hara, M. J. (2002). Plume-associated ultramafic magmas of phanerozoic age. *J. Petrol.*, 43:1857–1883.
- Kamenetsky, V. S., Sobolev, A. V., Joron, J. L., and Semet, M. P. (1995). Petrology and geochemistry of Cretaceous ultramafic volcanics from eastern Kamchatka. *J. Petrol.*, 36:637–662.
- Kerr, A. C., Tarney, J., Marriner, G. F., Nivia, A., and Saunders, A. D. (1997). The Caribbean–Colombian cretaceous igneous province: the internal anatomy of an oceanic plateau. In Mahoney, J. J. and Coffin, M. F., editors, *Large Igneous Provinces: Continental, Oceanic, and Planetary Flood Volcanism*, pages 123–144. American Geophysical Union, Washington, D.C.
- Larsen, L. M. and Pedersen, A. K. (2000). Processes in high-Mg, high-T magmas: evidence from olivine, chromite and glass in Palaeogene picrites from West Greenland. *J. Petrol.*, 41(7):1071–1098.
- Liu, B. P., Feng, Q. L., Fang, N. Q., Jia, J., and He, F. X. (1993). Tectonic evolution of Palaeo-Tethys poly-Island-ocean in Changning–Menglian and Lancangjiang belts, Southwestern Yunnan, China. *J. China Univ. Geosci.*, 18(5):529–539.
- MacLennan, J., Kenzie, D. M., and Gronvöld, K.

- (2001). Plume-driven upwelling under central Iceland. *Earth Planet. Sci. Lett.*, 194(1–2):67–82.
- McKenzie, D. and Bickle, M. J. (1988). The volume and composition of melt generated by extension of the lithosphere. *J. Petrol.*, 29:625–679.
- McKenzie, D. P., Jackson, J., and Priestley, K. (2005). Thermal structure of oceanic and continental lithosphere. *Earth Planet. Sci. Lett.*, 233:337–349.
- Milidragovic, D., Chapman, J. B., Bichlmaier, S., Canil, D., and Zagorevski, A. (2016). H<sub>2</sub>O-driven generation of picritic melts in the Middle to Late Triassic Stuhini arc of the Stikine terrane, British Columbia, Canada. *Earth Planet. Sci. Lett.*, 454:65–77.
- Niu, Y. L. (2004). Bulk-rock major and trace element compositions of abyssal peridotites: implications for mantle melting, melt extraction and post-melting processes beneath Mid-Ocean Ridges. *J. Petrol.*, 45:1–36.
- Pearce, J. A. (2008). Geochemical fingerprinting of oceanic basalts with applications to ophiolite classification and the search for Archean oceanic crust. *Lithos*, 100:14–48.
- Putirka, K. D. (2005). Mantle potential temperatures at Hawaii, Iceland, and the mid-ocean ridge system, as inferred from olivine phenocrysts: Evidence for thermally driven mantle plumes. *Geochem. Geophys. Geosyst.*, 6(5):1–14.
- Putirka, K. D. (2008). Thermometers and barometers for volcanic systems. *Rev. Mineral. Geochem.*, 69:61–120.
- Putirka, K. D., Ryerson, F. J., Perfit, M., and Ridley, W. I. (2011). Mineralogy and composition of the oceanic mantle. *J. Petrol.*, 52:279–313.
- Révilion, S., Arndt, N. T., Chauvel, C., and Hallot, E. (2000). Geochemical study of ultramafic volcanic and plutonic rocks from Gorgona Island, Colombia: the plumbing system of an oceanic plateau. *J. Petrol.*, 41(7):1127–1153.
- Rhodes, J. M. (1995). The 1852 and 1868 Mauna Loa picrite eruptions: Clues to parental magma compositions and the magmatic plumbing system. *Washington DC Amer. Geophys. Union Geophys. Monogr.*, 92:241–262.
- Roeder, P. L. and Emslie, R. F. (1970). Olivine-liquid equilibrium. *Contrib. Mineral. Petrol.*, 29:275–289.
- Schuth, S., Rohrbach, A., Munker, C., Ballhaus, C., Garbe-Schonberg, C., and Qopoto, C. (2004). Geochemical constraints on the petrogenesis of arc picrites and basalts, New Georgia Group, Solomon Islands. *Contrib. Mineral. Petrol.*, 148:288–304.
- Sobolev, A. V. and Nikogosyan, I. K. (1994). Igneous petrology of long-lived mantle plumes: the Hawaii (Pacific) and Reunion Island (Indian Ocean). *Petrology*, 2(2):131–168.
- Sun, S. S. and McDonough, W. S. (1989). Chemical and isotopic systematics of oceanic basalts: implications for mantle composition and processes. *Geol. Soc. Lond. Spec. Publ.*, 42(1):313–345.
- Thompson, R. N. and Gibson, S. A. (2000). Transient high temperatures in mantle plume heads inferred from magnesian olivines in Phanerozoic picrites. *Nature*, 407(6803):502–506.
- Thompson, R. N., Gibson, S. A., Dickin, A. P., and Smith, P. M. (2001). Early cretaceous basalt and picrite dykes of the Southern Etendeka Region, NW Namibia: windows into the role of the tristan mantle plume in paran–etendeka magmatism. *J. Petrol.*, 42:2049–2081.
- Walter, M. J. (1998). Melting of garnet peridotite and the origin of komatiite and depleted lithosphere. *J. Petrol.*, 39:29–60.
- Wan, Z. H., Coogan, L. A., and Canil, D. (2008). Experimental calibration of aluminum partitioning between olivine and spinel as a geothermometer. *Amer. Mineral.*, 93:1142–1147.
- Xu, Y. G., He, B., Chung, S. L., Menzies, M. A., and Frey, F. A. (2004). The geologic, geochemical and geophysical consequences of plume involvement in the Emeishan flood basalt province. *Geology*, 30:17–920.
- Zhang, F. and Feng, Q. L. (2002). Early carboniferous radiolarians in phosphoric nodule from Manxin, Menglian, Southwestern Yunnan. *Acta Micropalaeontol. Sin.*, 19(1):99–104.
- Zhang, S. Q. and Zhu, Q. W. (1995). Late Palaeozoic Volcanic Rocks in the Menglian Region, southwestern Yunnan. *Tethyan Geol.*, 19:21–37.
- Zhong, D. L. (1998). *The Paleotethyan Orogenic Belt in western Yunnan and Sichuan*. China Science Publishing and Media Ltd, Beijing.